

Energy characterization of buildings in polar climate: case study of *Gabriel de Castilla* Antarctic station

Beatriz Rodríguez Soria¹, Miguel Ángel García García¹, Adeline Rezeau¹

¹ CUD – University Defence Center, General Military Academy, Crtra. Huesca s/n, 50090
Zaragoza (Spain)

Corresponding author: arezeau@unizar.es

Keywords: energy consumption, indoor air conditions, thermal comfort, transmittance, air leakages, thermography, Antarctica

ABSTRACT

In this paper, we present the energy characterization of two habitable modules at the Spanish station “Gabriel de Castilla”, located on Deception Island, Antarctica. The analysis includes profiles of energy consumption for space heating and domestic hot water, as well as indoor air conditions, which were all recorded during one month of Antarctic summer. Additionally, the measurement of walls’ transmittance and air infiltrations, together with thermography analysis, enabled evaluating the conservation state of the buildings’ envelope. Upon analyzing all this data, it is evident that there is potential to enhance the design of future modules, improving the thermal comfort while significantly reducing the energy consumption. This will contribute to decrease the logistics and environmental impacts of these research stations, crucial considerations in human activity on the Antarctic continent.

1. INTRODUCTION

The building sector is currently undergoing a paradigm shift, driven by the need to reduce energy consumption and explore cleaner energy sources. The primary goal is to decrease greenhouse gas emissions, which are the main cause of atmospheric degradation and climate change on our planet.

This international concern has been addressed since 1997 with the approval of the Kyoto Protocol [1], [2], where common goals for reducing CO₂ emissions (based on quotas) and energy consumption were established globally to prevent adverse effects on the environment. The outcome, instead of promoting emission reduction in the most polluting countries, led to a market for buying and selling CO₂ between highly industrialized nations and those with less industry, and consequently, lower pollution. Recognizing that the limits set in the Kyoto Protocol were insufficient to mitigate climate change, they were revisited for the second commitment period that started in 2013, and new action proposals were outlined [3], [4]. Latter, in

31 2015, the Paris Agreement was adopted by 196 Parties at the UN Climate Change Conference (COP21) and
32 aims to limit the temperature increase to 1.5 °C above pre-industrial levels. Such agreement is a “landmark
33 in the multilateral climate change process” because, for the first time, a binding agreement brings all nations
34 together to combat climate change [5].

35 In 2016, the Climate Change Conference took place in Marrakech and ended up with an agreement that calls
36 for a significant boost of transparency of action, including for measuring and accounting emissions
37 reductions, the provision of climate finance, and technology development and transfer. An Action
38 Proclamation was also issued by heads of state, government, and delegations, to signal a shift towards “a
39 new era of implementation and action on climate and sustainable development” [6]. The governments
40 committed to complete a rule book for operationalizing the Paris Agreement by the 2018. More than 40
41 vulnerable nations even announced ambitious aims, including achieving 100% renewable energy between
42 2030 and 2050. The enthusiasm for the potential success of the proposed measures was overshadowed when
43 United States (US) president-elect declared that he would start measures to withdraw the country from the
44 Paris Climate Agreement. After several years out of the Paris Agreement, US officially rejoined it in 2021
45 and set an ambitious nationally determined contribution to reduce net greenhouse gas emissions by 50-52%
46 in 2030 [7]. In this line, the Climate Change Policy guide, approved by the American Planning Association
47 in 2020, advocates for a strong international leadership on climate change, with an ambitious goal of reaching
48 net-zero emissions by 2050 [8].

49 At European level, the Commission initially adopted in 2006 the Green Paper for a European Strategy for
50 Sustainable, Competitive and Secure Energy [9]. The main goal was to adopt an “integrated approach to
51 climate and energy policy that aims to fight climate change and enhance the energy security of the EU while
52 simultaneously boosting its competitiveness”. After adopting Paris Agreement and ratifying Doha
53 Amendment to Kyoto protocol, the European Commission confirmed its commitment to tackling climate and
54 environmental-related challenges with the publication of its strategic long-term vision “Clean Planet for all”
55 in November 2018 [10] and the adoption of the European Green Deal, in December 2019 [11]. By adopting
56 the latter, the EU and its member states committed to cutting net greenhouse gas emissions in the EU by at
57 least 55% by 2030, compared to 1990 levels, and to achieving climate neutrality by 2050.

58 Globally, countries all over the world have drafted national climate action plan to cut emissions and adapt to
59 climate impacts, i.e. Nationally Determined Contribution (NDC) under the Paris Agreement. So far, all 193
60 Parties to the Paris Agreement have issued at least a first NDC and 151 Parties communicated a new or
61 updated NDC as of 2 November 2021 [12]. In this way, each state or union of states has defined measures to
62 mitigate climate change in an ecological transition process, except in the case of the Antarctic continent.

63 The Antarctic continent contains about 90% of the world's ice and it reflects a large part of the solar radiation
64 it receives [13]. The warming and reduction of such ice area have a direct impact on marine and terrestrial
65 ecosystems on the planet [14], [15]. Moreover, the permanent frozen ground (permafrost) layer, which

66 underlies most of the Antarctic continent [16], is also threatened by global warming. As shown by many
67 studies, e.g. [17][18], permafrost thaw leads to the release of carbon emissions, with important consequences
68 on the intensification of climate change. For all these reasons, many researches are being carried out in the
69 so-called “continent of science” in order to better understand and predict the current state and the evolution
70 of Antarctic continent’s environment.

71 Obviously, human activities on the Antarctica continent are (up to now) much less intensive than other
72 countries and continents; but their impacts on the local environment and climate may be even or more critical.
73 In addition, no commitment had been yet agreed to set specific values for greenhouse gas emissions and
74 fossil-based energy consumption at Antarctic bases. Only environmental protection measures for fauna, flora
75 and marine environment, have been established [19]–[21], as well as national plans compiling the measures
76 taken by each country at their scientific bases, e.g., [22], [23].

77 In a previous study, De Pablo et al. [24] analyzed the potential effects of Antarctic station’s buildings on the
78 permafrost degradation. By monitoring the ground temperature and the thickness of the active layer, they
79 showed a degradation of the permafrost due to anthropic activity. They evidenced the station reduces the
80 freezing of the ground during the winter when the station is closed and facilitates the warming of the ground
81 during the living periods of the station in the Antarctic summer.

82 On the other hand, human activities also affect Antarctic environment through fuel usage and transportation
83 to provide energy to the stations. Even if the Deception Island Management Package [25] emphasizes the
84 importance of prioritizing energy efficiency (to minimize emissions at the station), almost no studies exist on
85 the actual efficiency of buildings used at Antarctic stations. Up to now, main interest has been focused on
86 producing energy based on renewable sources [26], implementing more efficient energy devices, or on
87 analyzing global environmental impacts. For example, S. Brooks proposed a standardized approach to
88 measuring the human footprint of research stations, by collecting information about building total surfaces,
89 location characteristics, type of construction and usage [27]. More recently, Crossin et al., presented the
90 environmental impacts of a case-study Antarctic station [28]. They applied a life cycle analysis and identified
91 that higher impacts were related to freight operations and electricity cogeneration.

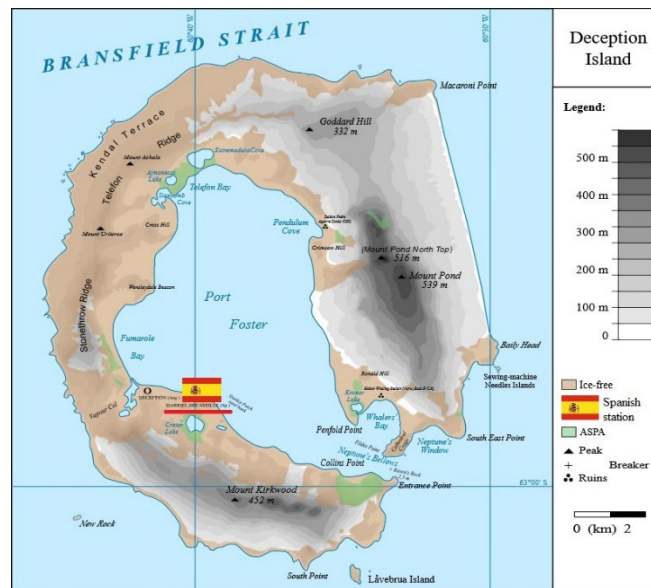
92 In the present research, we examine the thermal performance and energy consumption of the scientific station
93 “Gabriel de Castilla” (GdC from now onwards), situated on Deception Island. This study is the first step
94 towards achieving energy-efficient retrofitting of the GdC station. Analyzing the thermal envelope and the
95 actual energy consumption of the existing buildings is crucial for effectively implementing a renovation
96 strategy of the station and establishing the basis for the construction of new modules that prioritize nearly
97 zero emissions, improved functionality and enhanced comfort. As highlighted in existing literature, such as
98 [29], [30], a comprehensive and detailed understanding of the factors influencing energy usage is essential
99 for achieving substantial improvements in energy efficiency of buildings. These factors include buildings
100 attributes, human behavior, energy systems, building maintenance, and other relevant aspects.

101 In the present paper, we present the results of energy consumption in the GdC scientific station during the
102 austral summer, along with a comprehensive characterization of the buildings' thermal envelope. These tasks
103 presented significant challenges, given the extreme climate conditions, the logistical issues and the inherent
104 difficulties associated with collecting data from occupied buildings. Our methodological approach involved
105 individualized and non-invasive techniques, and included walls' transmittance measurement, as well as
106 simultaneous blower door tests with thermography analysis.

107 2. MATERIALS AND METHODS

108 2.1. THE "GABRIEL DE CASTILLA" STATION

109 The GdC station is a scientific base that was inaugurated in 1989 and operates exclusively during the austral
110 summer, typically from November to March. The station is situated on Deception Island, in the South
111 Shetland archipelago, approximately 110 km north of the Antarctic Peninsula and roughly 1000 km away
112 from the South America continent. Most of the island is not covered by snow during austral summer (see ice-
113 free areas in Fig. 1) which, together with the exceptional and unique natural ecological system of the area,
114 makes it of great interest for scientific studies, including geological, fauna and flora, geodesic, geothermal,
115 and permafrost studies [23].

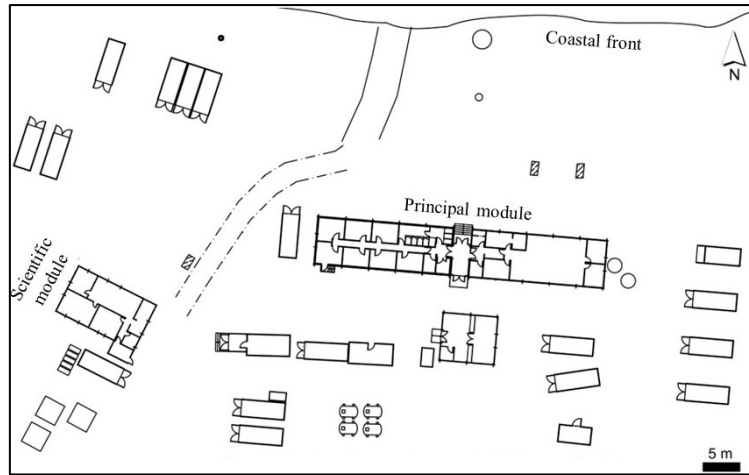


116

117 **Figure 1.** Map of Deception Island, adapted from [31]. ASPA: Antarctic Specially Protected Area.

118 The GdC station consists of a modular design featuring twenty-five distinct buildings or "modules". Figure
119 2 provides a map displaying the different buildings of the station. These include a scientific module, a
120 principal module, a nautical module, warehouses, an incinerator, a mechanical workshop, fuel tanks and a
121 septic tank, among others. To provide the station's energy needs, two diesel generators sets are utilized,
122 supplying electricity for lighting, scientific equipment, communications, water pumping, purification and
123 heating, as well as waste systems.

124 During the 2018-2019 Antarctic campaign, a comprehensive thermal performance assessment was conducted
125 on a majority of the buildings within the station. Notwithstanding, the present paper specifically concentrates
126 on the analysis of two main modules: the principal module and the scientific module (see Figure 2).
127 Subsequent sections provide a description of these modules.



128
129 **Figure 2.** Map of Spanish scientific station “Gabriel de Castilla” [32].

130 2.1.1. The principal module

131 The principal module is composed by two different wings, i.e., the “living” wing and the “bedroom” wing,
132 which are two structures of independent construction, connected by a main hall. These constructions are
133 improved TYCE 6.5/92 Barracks, with dimensions of 18.5 m x 6.5 m, which makes an area of 120.25 m² for
134 each one [24]. The structure raises from the ground using galvanized steel pillars. These pillars support a
135 lattice metal structure, which in turn supports the roof's truss system. The entire structure is protected with
136 anti-rust and lacquered paints. The flooring is made of water-resistant particle board, with a vapor barrier
137 consisting of a corrugated aluminum sheet, a polyethylene film, and a 6 mm thick PVC tile. The vertical
138 enclosure is composed of sandwich panels. The interior part of the panels contains fiberglass wool with a
139 vapor barrier made of an aluminum sheet. The exterior carpentry is made of lacquered aluminum with thermal
140 break and Climalit-type double-glazed windows. The roof is also constructed with a sandwich panel and
141 polyurethane insulation.

142 It is important to highlight that the bedroom wing has been specifically designed and constructed for the GdC
143 base, while the living wing was already in use in Spain and has been transported to Antarctica.

144 With respect to the living wing, its interior distribution provides a kitchen, living-dining room, transmission
145 room and an office room (see Figure 4). Moreover, two small utility rooms are located next to the entrance
146 room, one for an electric tank-type storage water heater and the other for a gasoil hot air furnace. The electric
147 heater has a nominal power of 1.4 kW_e (230 V 1 ph.) and provides instantaneous domestic hot water (DHW)
148 for the kitchen. On the other side, the furnace's nominal power is 34,500 kcal/h (~ 40 kW_{th}), plus the electric
149 consumption for the furnace blower, and the nominal air flow is 2,650 m³/h [24]. Heating control is based on

150 an integrated thermostat that causes the furnace to turn on when the ambient air temperature decreases below
151 21°C. Finally, the hot air is distributed to the living wing by a duct system located in the ceilings, without any
152 mechanical ventilation system.

153 As regards the bedrooms wing's interior distribution, it provides a bathroom, a washer and dryer room, seven
154 bedrooms, as well as two small utility rooms (see Figure 4). Each bedroom includes four beds, which, together
155 with the kitchen and fuel capacities, limits the capacity of the GdC station to a maximum of 28 persons. As
156 for the living wing, heating is provided by a separated gasoil hot air furnace, with same nominal power and
157 thermostat set temperature. With respect to DHW, it is produced thanks to an electric tank-type heater, with
158 a nominal power of 5.1 kW_e (400 V 3 ph.).

159 2.1.2. Scientific module

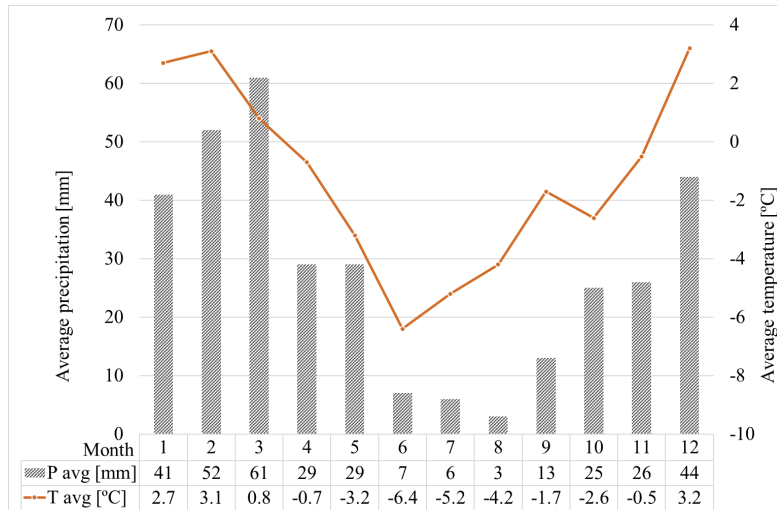
160 This module is designated as office space for the scientific staff working at the station during the Antarctic
161 summer. Its structure is made by standard 20' containers that were assembled so as to obtain a total surface
162 of 90 m². The scientific module was designed for its specific use in the Antarctic station and it includes a
163 reinforced insulation and double-glazed windows. As can be seen in Figure 4, the layout comprises a main
164 room and three individual offices.

165 In terms of energy demand, the scientific module does not have DHW and typically requires heating only
166 during the working hours. For this purpose, a portable electric fan heater is available in the main room, with
167 nominal power of 5 kW_e (400 V 3 ph.) and a manual switch on/off. Additionally, two electric radiators are
168 used to provide heat through convection in the office n°2. These radiators have a nominal power of 2.8 kW_e
169 (230 V 1 ph.) and operate with a thermostat and adjustable temperature settings.

170 2.2. METEOROLOGICAL DATA

171 The climate of Deception Island is polar maritime [25] and over 57 % of the island is covered by permanent
172 glaciers. The latitude and the longitude of the site are respectively 62°57'S and 60°38'W. The GdC station is
173 located in an area between 50 m and 100 m from the sea and on an ice-free ground. Nevertheless, the overall
174 island, including the station, is covered by snow during the winter.

175 Since 2005, the Spanish State Meteorological Agency operates an autonomous weather station in the GdC
176 Antarctic base [33]. According to the absolute values recorded from 2005 to 2020, the mean annual air
177 temperature over those years was -1.2 °C, with a maximum air temperature of 13.3 °C (in February 2020) and
178 a minimum air temperature of -22.5°C (in July 2007). Yearly precipitation and temperature are depicted in
179 Figure 3. Daily averaged wind speeds during the 2000 ranged from 0.2 m/s in October to 47.4 m/s in June,
180 with the prevailing direction from the southwest and, less frequently, blowing from the northeast [33], [34].
181 The winds blowing bring humidity to the area (mean relative humidity around 80 %) and they transport
182 pyroclastic particles, which may damage the buildings' envelope by abrasion.



183

184

185

Figure 3. Yearly precipitation and temperature at GdC weather station, from 2005 to 2020 (data from [33]).

186

2.3. MONITORING SENSORS AND METHODOLOGY

187

188

189

190

In order to analyze the thermal behavior and comfort conditions in GdC station, real-time electricity consumption data and indoor air conditions data were recorded during the Antarctic 2018/2019 campaign. In the present paper, emphasis is made to the monitoring period comprised between February 15th and March 14th 2019. The following data were monitored:

191

192

193

194

195

196

197

198

199

- Temperature, relative humidity and CO₂ concentration were registered each hour in both the principal and the scientific modules by Wöhler CDL 210 CO₂ loggers.
- Temperature and relative humidity were registered at five different points thanks to HOBO UX100 data loggers. Two of them were fixed at the same place in the living room, but different height¹ (0.1 m and 1.7 m) in order to analyze the thermal gradient in the room.
- Apparent power (kVA) and active power (kW) of the heating and DHW systems were measured using electric network analyzers. The PCE-PA 8000 model was utilized for measuring the consumption of 3-phases devices, while the Voltcraft 4000 energy loggers were used for monophasic systems.

200

201

202

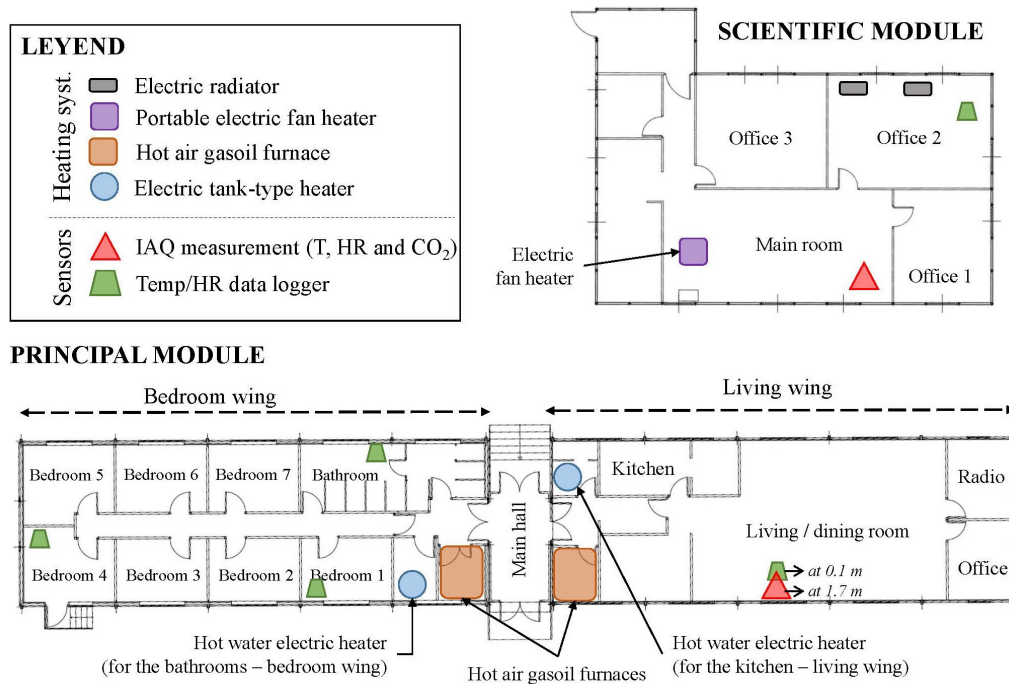
203

204

205

The data obtained from the energy analyzers and loggers was utilized to calculate the total energy consumption. Additionally, the gasoil consumption for the two hot air furnaces was measured using a flow meter over the course of an entire day. Figure 4 and Table 1 indicate the placement and name of each sensor utilized in the present study. The selection of monitoring points was based on various factors, including the specific usage of each room, the orientation of windows in relation to the cardinal directions, and the characteristics of the building envelope.

¹ According to ISO 7726:1998 [11] - Table 5: “recommended heights to measure physical quantities of an environment”.



206
207 **Figure 4.** Layout of the modules and location of the sensors and energy systems.

208 **Table 1.** Summary of the monitoring sensors and their location.

Sensor location	Temperature [°C]	Relative Humidity [%]	CO ₂ concentration [ppm]	Source
Exterior	T_{ext}	RH_{ext}	-	[33]
Scientific module - Main room	T_{sc1}	RH_{sc1}	$CO_{2,sc1}$	Wöhler logger
Scientific module - Office 2	T_{sc2}	RH_{sc2}	-	HOBO logger
Principal module - living room (1.7 m)	T_{lf}	RH_{lf}	$CO_{2,lf}$	Wöhler logger
Principal module - living room (0.1 m)	$T_{lf_0.1m}$	$RH_{lf_0.1m}$	-	HOBO logger
Principal module - Bedroom 1	T_{br1}	RH_{br1}	-	HOBO logger
Principal module - Bedroom 4	T_{br4}	RH_{br4}	-	HOBO logger
Principal module - Bathrooms	T_{bath}	RH_{bath}	-	HOBO logger

209 Furthermore, the conservation status of the buildings was assessed based on three key factors: the actual wall
210 transmittance, the extent of air leakage and the presence of thermal bridges. The global transmittance of the
211 enclosures was measured using the Testo 435 transmittance meter. To obtain these measurements, data was
212 collected for one hour, with measurements taken every minute, in various areas of the external walls. Each
213 area measured at least one square meter. Measurements were taken away from windows or corners to avoid
214 interference from thermal bridges. Additionally, areas unaffected by possible air currents were chosen to
215 maintain the accuracy of the average heat convection coefficient used in the calculation.

216 To quantify air leakages within the buildings joints, a blower door test was performed at 50 Pa, using the
217 RETROTEC Blower Door 311 LCP DM32 equipment. This test was conducted following the specifications
218 outlined in ISO 9972:2019 [35]. Simultaneously, thermography analysis was carried out using a Flir

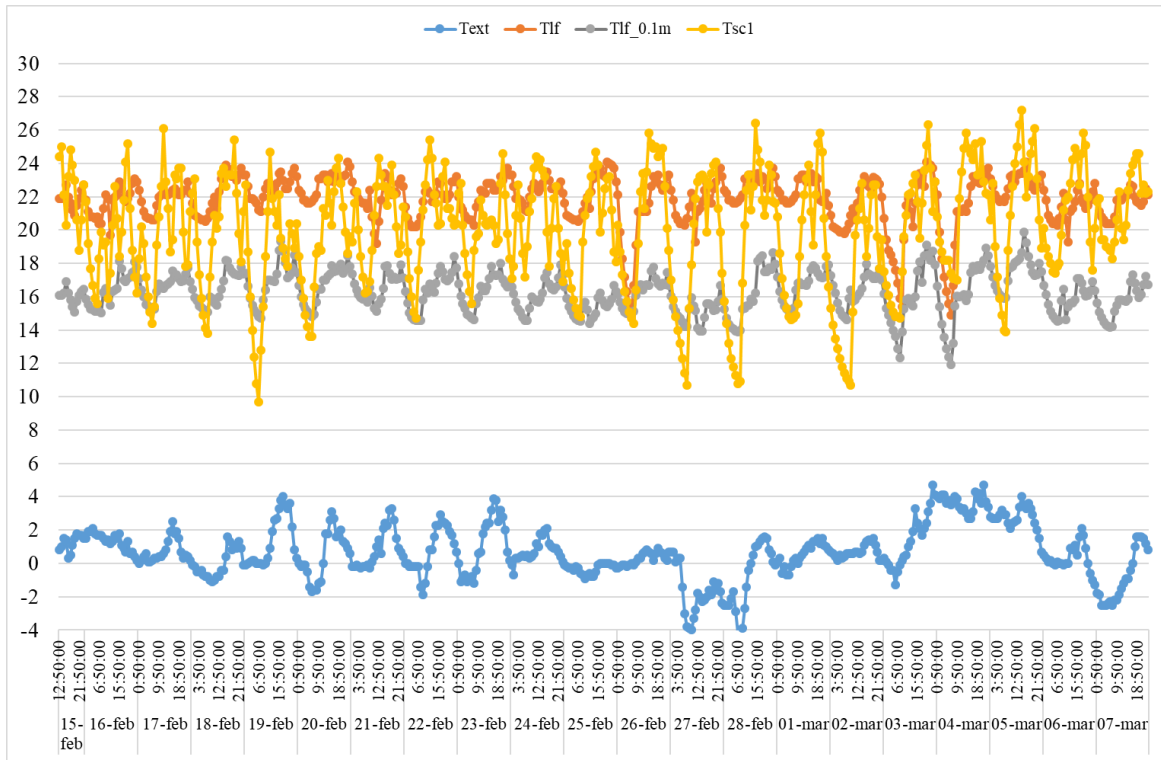
219 thermographic camera. This analysis helped identify hot/cold spots and thus detect potential thermal bridges
220 and air leaks in the building envelope.

221 3. RESULTS AND DISCUSSION

222 3.1. INDOOR AIR CONDITIONS (T , RH AND CO_2)

223 3.1.1. Air temperature and relative humidity

224 Ambient air temperatures measured in the scientific and the principal modules are illustrated in Figure 5,
225 specifically for the first three weeks of the monitoring period. The exterior climatic conditions are also
226 presented, based on the weather station data. Throughout the four-week monitoring period, the exterior
227 temperature fluctuated between -4°C and 4.7°C , with an average exterior temperature of 0.7°C . In terms of
228 indoor temperatures, they followed a cyclic pattern characterized by daytime increases leading to a peak
229 around solar midday, followed by nighttime decreases reaching minimum values. Although this cyclic trend
230 was anticipated, a significant difference was observed in the daily temperature variation between the scientific
231 module and the living wing. For instance, on February 28th, the scientific module (T_{sc1}) exhibited a variation
232 of 15.5°C , whereas the variation in the living wing (T_{lf}) was less than 2°C on the same day. Furthermore, it
233 should be noted that the ambient temperature in the principal module experienced substantial decreases during
234 certain nights. For instance, on February 26th and March 3rd and 4th, the temperature at a height of 1.7 m
235 dropped to minimum values below 17°C . These daily variations in temperature are primarily attributed to
236 the utilization of the heating system in each module, as well as the insulation properties of their respective
237 envelopes and the potential presence of thermal bridges. These aspects are analyzed later in sections 3.2 and
238 3.3. It is assumed that the impact of radiation is low, given that the incoming solar radiation is scarce due to
239 the sun's low position on the horizon in this region of the world.



240

241

242

Figure 5. Comparison between the outdoor temperature and the temperatures recorded in the living room at two different heights (0.1 m and 1.7 m) as well as in the main room of the scientific module.

243

244

245

246

247

248

249

250

251

252

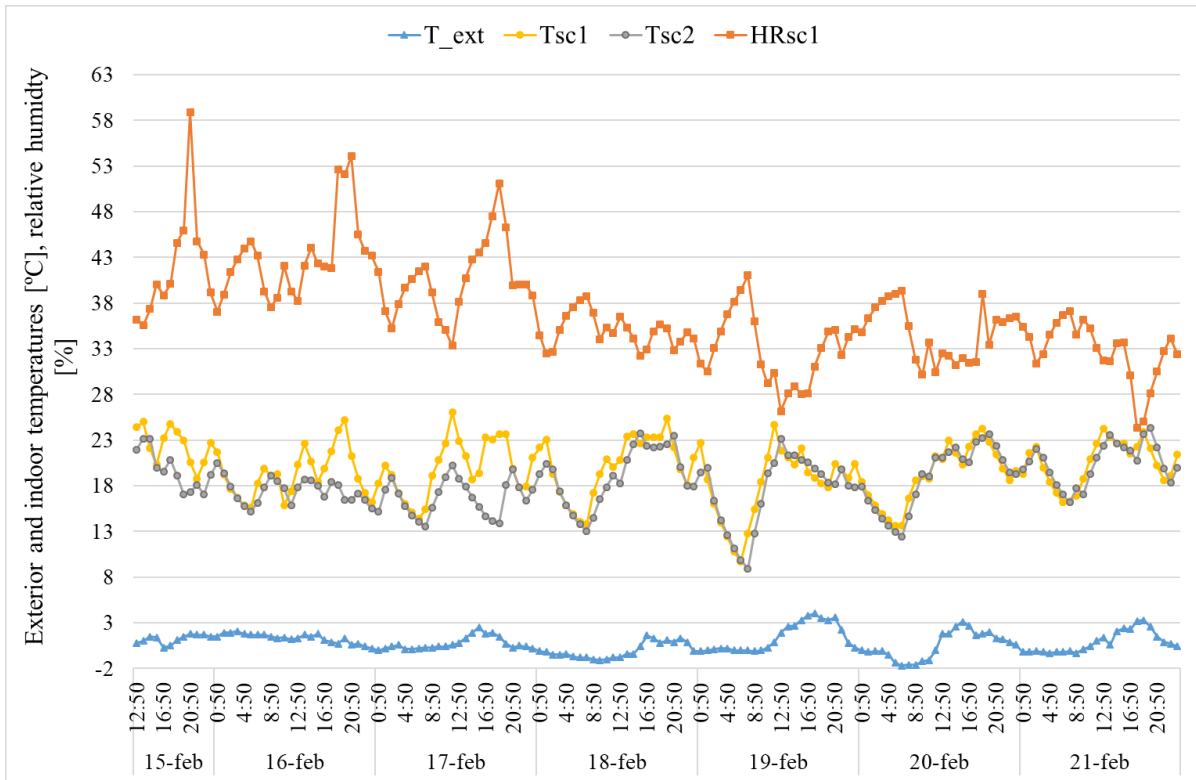
253

254

255

256

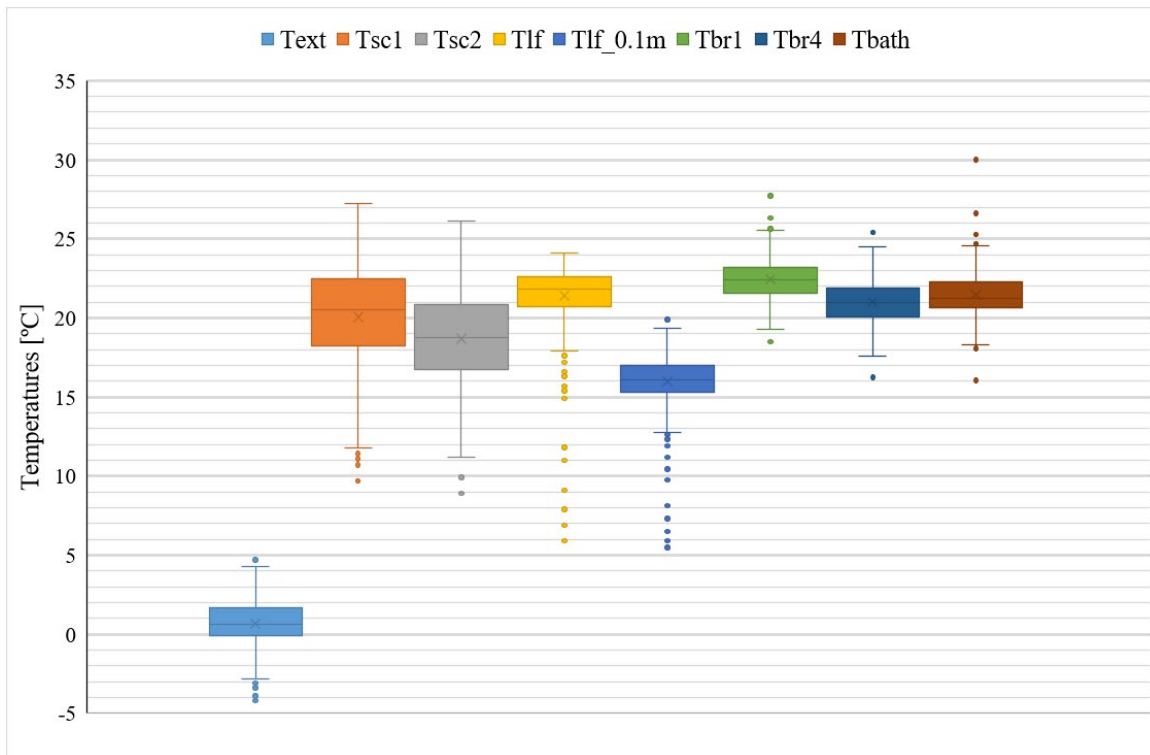
Figure 6 illustrates a comparison between the ambient temperatures in the main room (T_{sc1}) and in the second office (T_{sc2}) of the scientific module, alongside with the exterior temperature and relative humidity, for the first monitoring week. It can be observed that the main room generally had higher temperatures compared to the second office. This difference was particularly pronounced on February 16th, with a registered difference of 8.7 °C at 19:50, and on February 17th where a difference exceeding 8.6 °C was measured during three consecutive hours in the afternoon. In terms of weather data, these days coincided with wind velocities exceeding 20 km/h and a prevailing wind direction from the southwest. Considering the location of the offices, see Figure 3 and Figure 4, the second office is more exposed to wind compared to the main room of the scientific module. This exposure may have resulted in additional air leakages or infiltration, leading to a lower ambient temperature in the second office. When considering the entire monitoring period, similar behavior is observed and the average temperatures were 20.1 °C in the main room and 18.7 °C in the second office, as depicted in Figure 7. Instances where the temperature fell below the minimum comfort threshold of 17 °C [36], [37] [38] were mainly observed during the nights, when the scientific module was unoccupied and the heating systems were turned off.



257
 258 **Figure 6.** Comparison between the exterior temperature and the thermal conditions in the scientific
 259 module during the first week of monitoring.

260 Figure 7 provides a summary of the temperatures recorded at the seven monitoring points using a box and
 261 whisker plot. The middle line within the box represents the median temperature over the entire monitoring
 262 period, while the cross represents the arithmetic mean. The box represents the interquartile range, indicating
 263 the statistical spread of the data within the middle 50%. From this graphical summary, it can be observed that
 264 the temperatures in the scientific module exhibit the largest disparity or spread. These findings align with the
 265 observations depicted in Figure 5, which shows significant daily variation of temperature. Regarding the
 266 temperature profile in the “living” wing, a notable difference is observed between the ambient temperatures
 267 at 1.7 m (T_{lf}) and 0.1 m ($T_{lf_{0.1m}}$). Considering the complete monitoring period, the average temperature
 268 difference is 5.4 °C, which exceeds the 2 °C limit set by European standards [38], and shows a large
 269 discomfort. Overall, it is observed that more than 50% of the measured data in the living room at 0.1 m
 270 ($T_{lf_{0.1m}}$) fell below the minimum comfort temperature of 17°C. Several factors contribute to this result,
 271 including the characteristics of the heating system, the air circulation and infiltrations, and the conservation
 272 status of the thermal envelope.

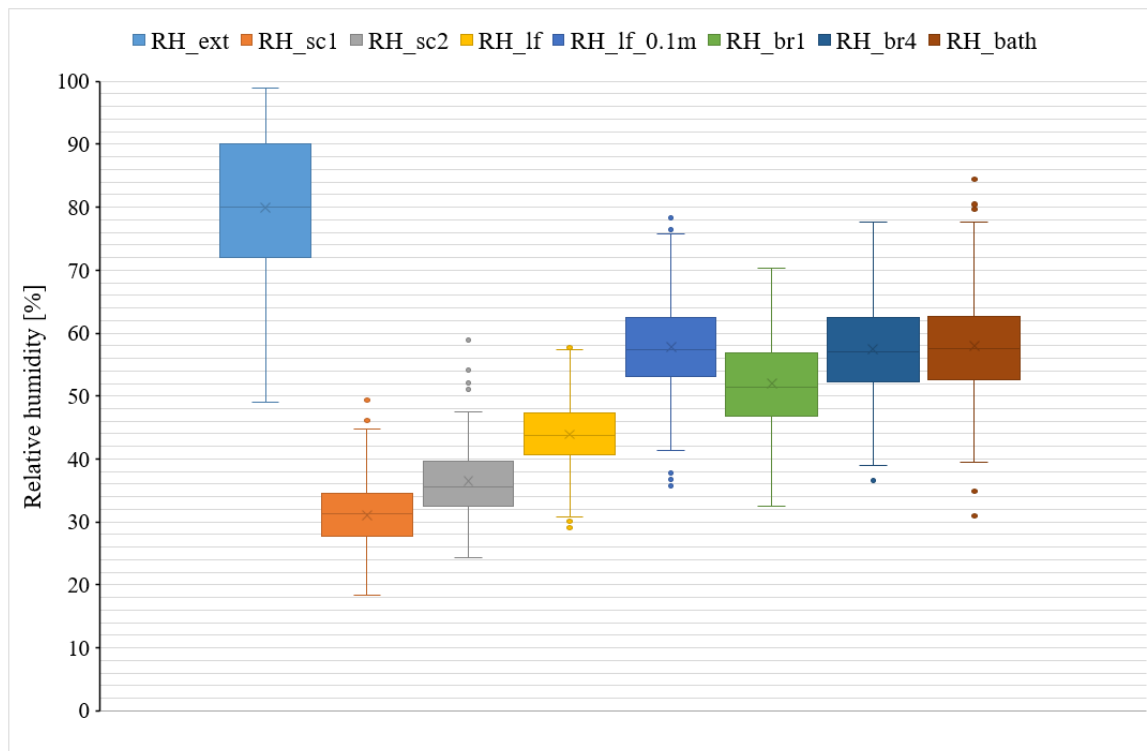
273 Considering bedrooms 1 and 4, a temperature difference of 1.4 °C is observed between their respective
 274 average values. This can be attributed to the location of each bedroom: bedroom 4 is situated on the corner
 275 of the module, exposed to prevailing winds, while bedroom 1 is adjacent to the boiler room and the bedroom
 276 2, which reduces heat losses to the exterior (see Figure 4). Overall, the temperatures in all bedrooms were
 277 above the minimum comfort temperature of 17°C, with only a few outliers falling below this threshold.



278
279
280

Figure 7. Summary of indoor air temperatures at the seven monitoring points, during the monitoring period.

281 Regarding the relative humidity, Figure 8 presents a visual overview of the measurements taken at the seven
 282 monitoring points. Significant variations are observed at each monitored point, as well as in the outdoor
 283 conditions. This result may also be observed in Figure 6. Noteworthy differences exist not only between
 284 modules, but also within the same area at different heights. For instance, variations are evident between the
 285 living room at 1.7 m and 0.1 m. Over the entire monitoring period, the scientific module and the living wing
 286 at a height of 1.7 m exhibited the lowest relative humidity values on average. These recorded humidity levels
 287 fall outside the recommended comfort range established by both the Spanish regulation [37] and the EN
 288 16798-1 standard [38], which has a more permissive threshold. Low relative humidity levels of this nature
 289 have been found to have negative effects on human health, including symptoms such as irritation of eyes and
 290 upper airways [39]. This aligns with the discomfort reported by the station staff members, who specifically
 291 mentioned dry throat and nose, as well as eyes irritation. On the other hand, the highest relative humidity
 292 values were observed in the living wing at 0.1 m and in the bathrooms. The latter is expected given their
 293 function, and the measured values fall within the anticipated range. However, in the living wing, such high
 294 relative humidity values may lead to water condensation, increase the risk of mold growth, and potentially
 295 impact the building structure's condition, as already reported in numerous studies, e.g., [40][41][42][43].



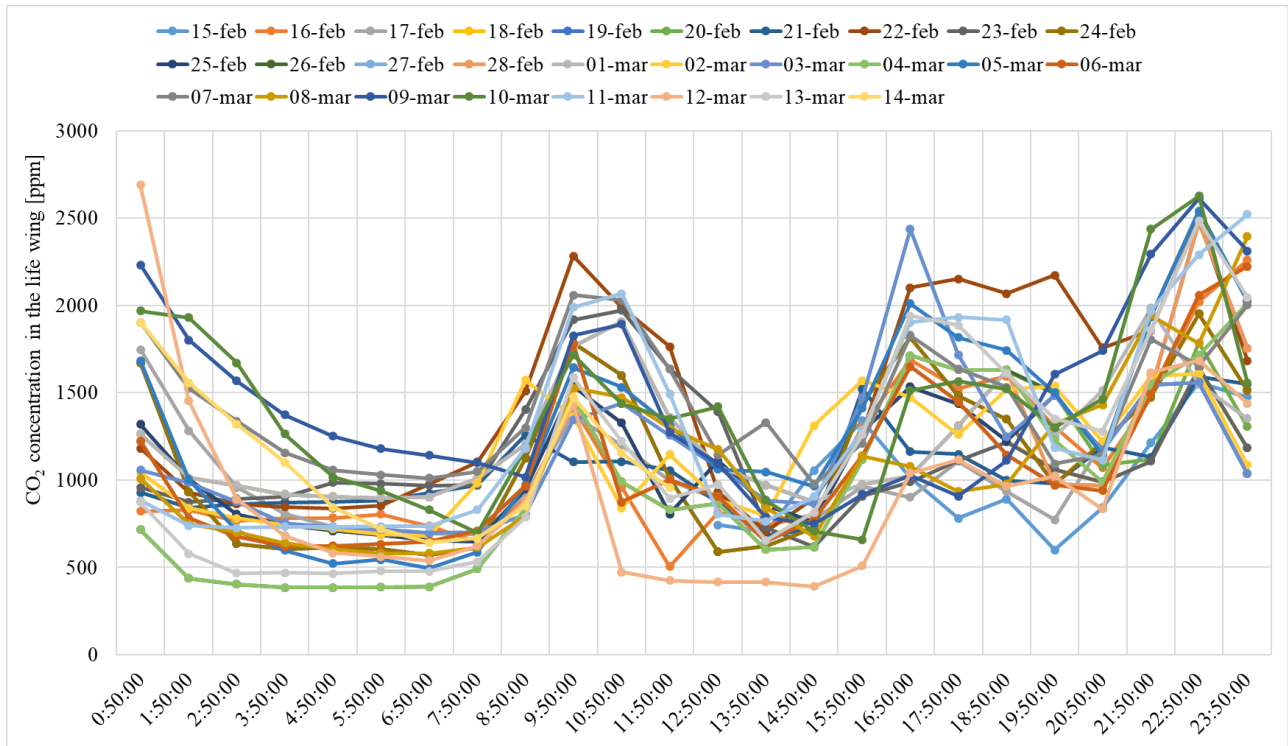
296
 297 **Figure 8.** Summary of indoor air relative humidity in the seven monitoring points, during the
 298 monitoring period.

299 3.1.2. CO₂ concentration

300 Figure 9 illustrates the daily variation of CO₂ concentration in the living/dining room of the living wing
 301 throughout the entire monitoring period. It is important to note that this room serves as the dining area for the
 302 staff, where breakfast, lunches and dinners are taken every day. The graph shows that the CO₂ concentration
 303 followed a periodic trend, characterized by three main peaks during the day:

- 304 • The first peak occurred from 8 am to 10 am, corresponding to the breakfast period.
- 305 • The second peak was observed from 3 pm to 5 pm, coinciding with the lunchtime at the station.
- 306 • The third peak took place from 9 pm to 11 pm, which was aligned with the coordination meeting and
 307 dinner time.

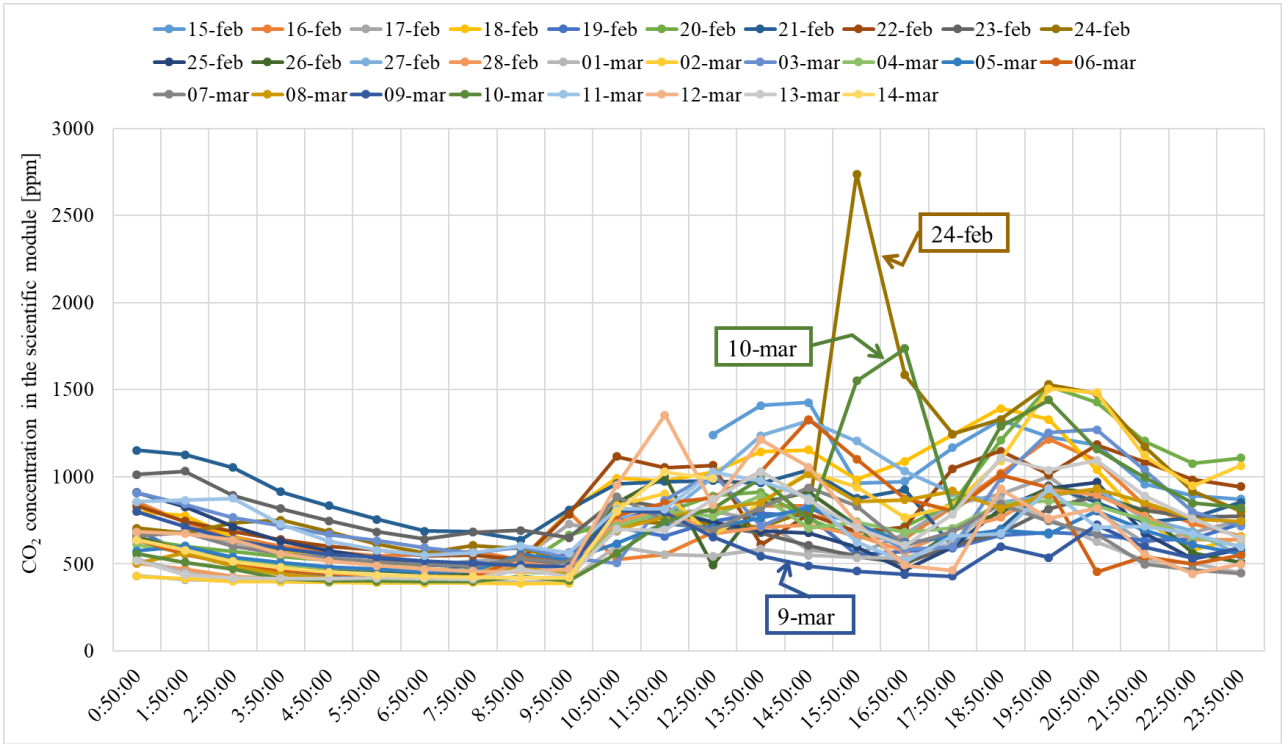
308 Following breakfast, the CO₂ concentration typically decreased due to the ventilation during morning
 309 cleaning activities. However, there was no ventilation conducted after lunch and throughout the afternoon.
 310 Consequently, with high occupancy in the living room for extended periods, the CO₂ concentration reached
 311 very high levels, surpassing 1,500 ppm, until 11 pm when the staff retired to bed. During the night, when the
 312 living wing remained unoccupied, the CO₂ levels slightly decreased to around 500-1,000 ppm. Overall, values
 313 exceeding 1,000 ppm were consistently measured for several consecutive hours in the living room of the
 314 principal module, highlighting a lack of air renovation and poor air quality.



315
316 **Figure 9.** Daily variation of CO₂ concentration (in ppm) in the living/dining room.

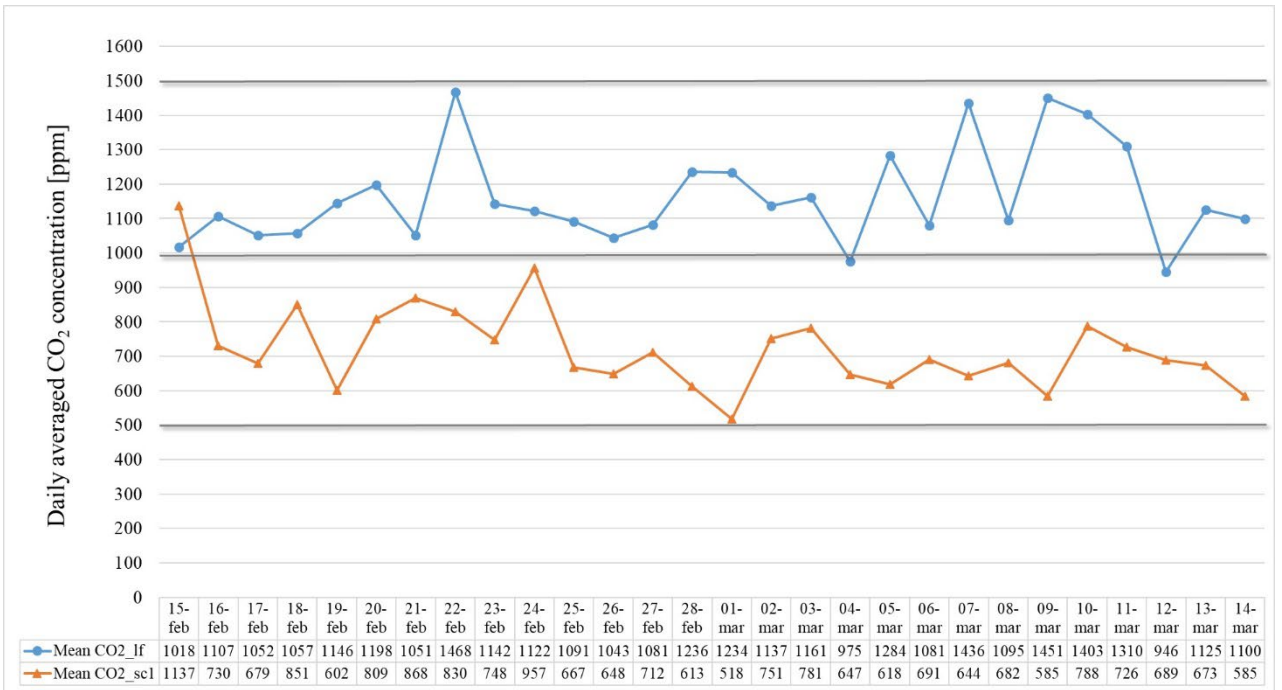
317 Figure 10 presents the daily variations of CO₂ concentration in main room of the scientific module throughout
 318 the entire monitoring period. The CO₂ concentration displays similar patterns for the early morning hours
 319 (from midnight until 9 am) across different days of the week. However, differences can be observed between
 320 days during working hours, i.e., approximately from 9 am to 9 pm. The CO₂ concentration in the main room
 321 varied between 500 ppm up to 1,500 ppm, depending on the activities carried out, and no significant peaks
 322 were observed, except for a couple of outliers' points on February 24th. It is worth noting that, in the case of
 323 the scientific module, the number of users was much lower and they were attentive to the CO₂ concentration
 324 readings on the CDL 210 logger and opened the windows when values exceeded 800 ppm. Accordingly, the
 325 profile of CO₂ concentration is relatively constant during working hours, but indoor temperatures present
 326 significant variations.

327 Additionally to the comparison of daily variations presented in Fig. 9 and 10, values of daily average depicted
 328 in Figure 11 allow observing the significant disparities among both buildings. The results indicate a moderate-
 329 to-low air quality in the living room of the principal module, while the scientific module presents a moderate
 330 air quality, as per the Spanish Regulation for Thermal Installations in Buildings [36], [37]. A low air quality
 331 may directly affect the well-being of the occupants, leading to symptoms such as headaches, general
 332 discomfort, and difficulties in concentration, among others. These effects have been widely recognized in
 333 existing literature [44]–[46], although existing evidence for these direct impacts on health is not always
 334 consistent and further research is recommended [47].



335
336

Figure 10. Daily variation of CO₂ concentration (in ppm) in the scientific module.



337

Figure 11. Daily average of CO₂ concentration in the living wing and in the scientific module.

338
339

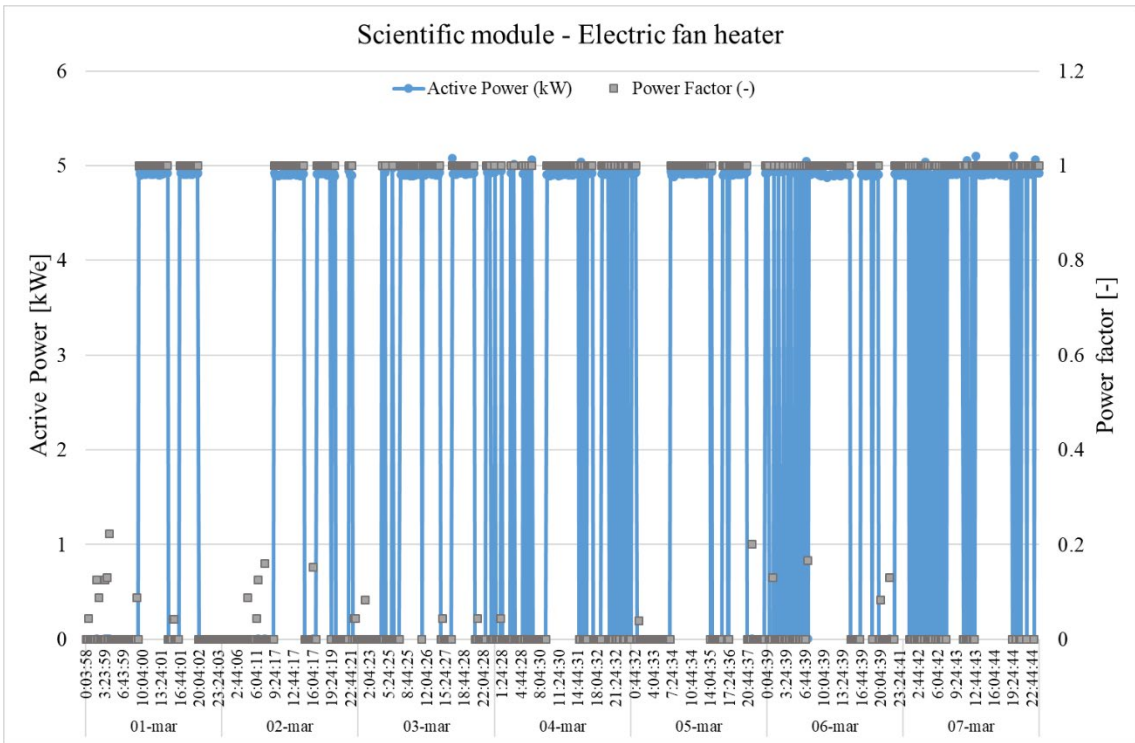
3.2. ENERGY CONSUMPTION

340 The real-time electric consumption of heating and DHW appliances was monitored over a period of four
341 weeks. The results presented in this section are analyzed separately based on the specific end-use of each

342 appliance. The energy consumed for lighting and other appliances are not considered in the scope of the
343 present study.

344 3.2.1. Energy consumption for heating purposes

345 In the scientific module, one portable electric fan heater was utilized to provide heating for the main room.
346 The operation of the heater relied on manual switching on and off by the staff members working in that
347 module. Figure 12 illustrates the active power and power factor of the fan heater during the third week of
348 monitoring. It can be observed that the mean power factor is 1 when the fan heater is operating, indicating
349 that it is a purely resistive device. Based on the operation profile shown in Fig. 12, we can not discern a
350 specific daily pattern. Although the heater was almost continuously in use in the morning (i.e, 9 am to 3 pm),
351 the operation was irregular during the afternoons, depending on the scientific activities that took place. During
352 the nights, the fan heater was usually turned off, except in cases when staff members worked overnight to
353 monitor volcano activity, for example. Throughout the entire monitoring period, the average daily usage time
354 of the fan heater amounted to 12.92 hours per day, which is considered quite high.

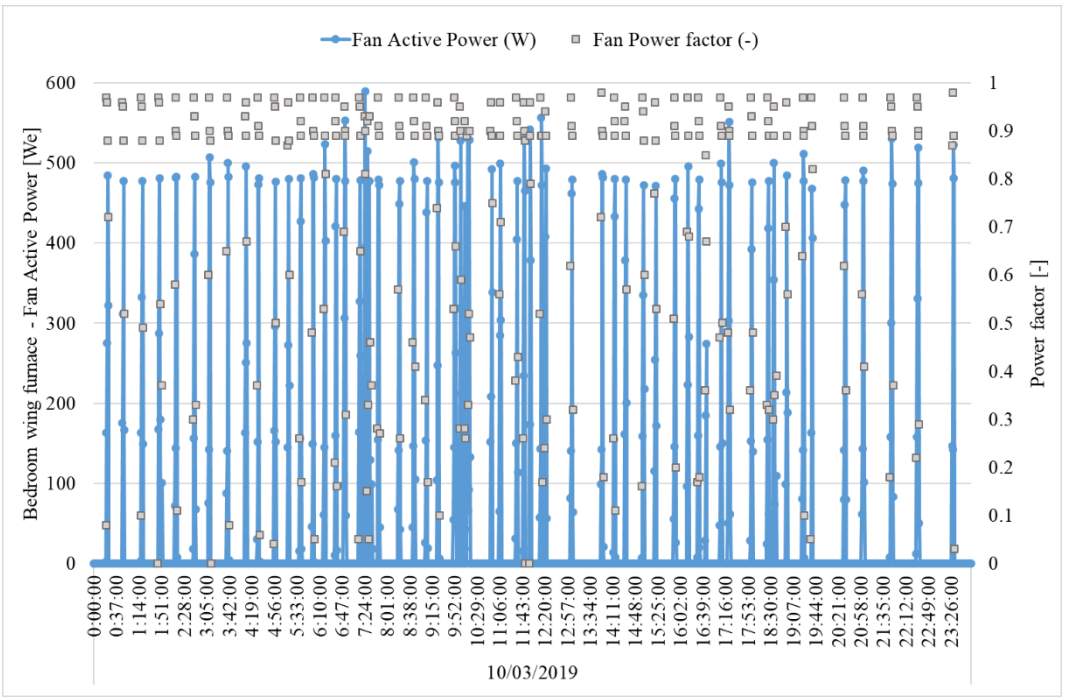


355
356 **Figure 12.** Operation profile of the electric fan heater in the main room, scientific module (3rd week).

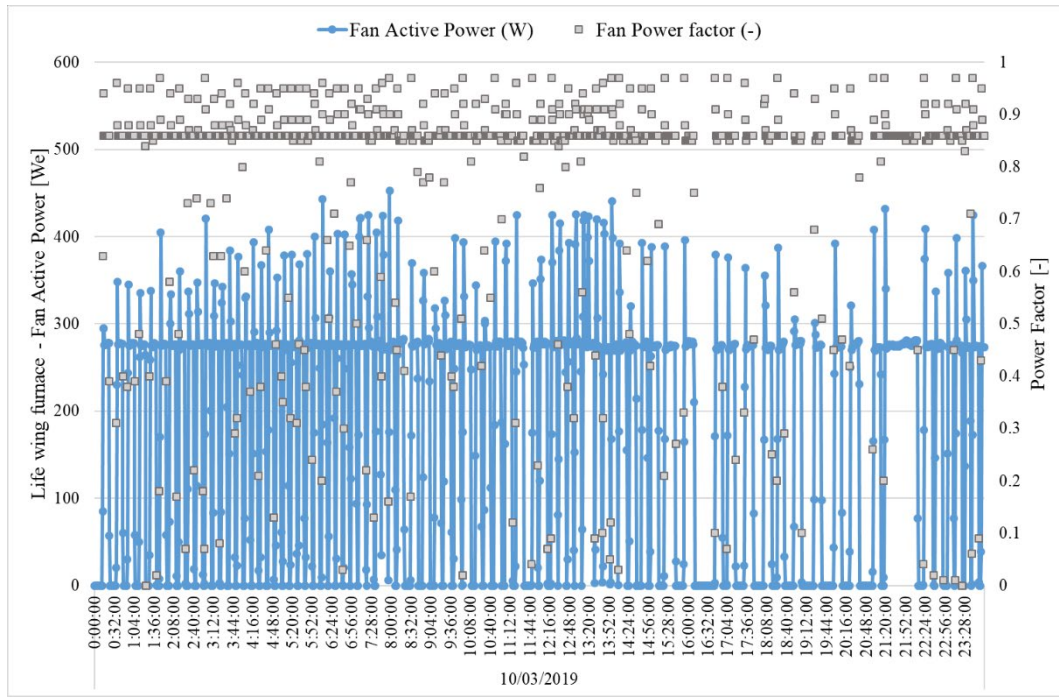
357 The relationship between the active power of the electric fan heater and the indoor temperature of the
358 scientific module is depicted in additional diagrams in the Appendix (see Fig. A1). As expected, the operation
359 of the heater has a direct impact on the indoor temperature. When the fan heater is turned off, the temperature
360 decreases linearly at a rate of approximately 2°C per hour. This observation suggests that the scientific module
361 has a relatively low thermal inertia.

362 In the principal module, two gasoil furnaces are responsible for providing hot air to the living and the bedroom
 363 wings. Both furnaces are equipped with integrated thermostats set at a fixed temperature of 21°C. The gasoil
 364 mass flow rate was measured for an entire day, resulting in an average consumption of 2 kg of fuel per hour
 365 of operation. Additionally, the electric consumption of each furnace's blower was measured using Voltcraft
 366 4000 energy loggers, as described in section 2.3. The active power and power factor are presented in Figure
 367 15 and in Figure 16 for the bedroom wing and the living wing, respectively. For convenience, the data is
 368 shown for a single monitoring day (March 10th). Both figures illustrate the frequent start/stop cycles
 369 throughout the day, with the furnaces operating for very short periods. Over the entire monitoring period, the
 370 bedroom wing's furnace had between 50 and 110 start/stop cycles per day, while the living wing's furnace
 371 had between 105 and 150 cycles per day.

372 When operating under stable conditions, the power factor of both fans was approximately 0.95. However,
 373 during the startup, the power factor dropped significantly, typically less than 0.8. The average power factors
 374 for the bedroom and the living wings blower over the entire monitoring period were 0.68 and 0.80,
 375 respectively. The power factor for the living wing blower is relatively higher due to its longer operating
 376 periods, as shown in Figure 14. On average, the bedroom wing furnace operated for 6.52 hours per day, while
 377 the living wing furnace operated for 17.15 hours per day, nearly three times higher. Despite both wings using
 378 the same furnaces and thermostat regulation, this discrepancy in operating times may be partly attributed to
 379 poorer insulation in the living wing. This aspect is further analyzed in section 3.3 through thermal imaging
 380 and envelope transmittance measurement.



381
 382 **Figure 13.** Operation profile of the furnace's blower (bedroom wing), during one day (10/03/2019).



383
384 **Figure 14.** Operation profile of the furnace's blower (living wing), during one day (10/03/2019).

385 3.2.2. Energy consumption for DHW purposes

386 In the principal module, two electric tank-type heaters were utilized for DHW purposes. The first heater,
387 located in the bathroom of the bedroom wing, has a power rating of 5.1 kW_e (3-phases), while the second,
388 smaller heater was installed in the kitchen with a power rating of 1.4 kW_e (1-phase). The DHW heater in the
389 bedroom wing was typically used for 2 or 3 cycles per day, primarily in the morning (between 7-10 am) and
390 in the evening (between 8 and 10 pm). During operation, it consumed an active power was 5.1 kW, indicating
391 a purely resistive load with a power factor of 1. On average, the DHW heater of the bedroom wing operated
392 for 3.77 hours per day, resulting in a total energy consumption of 531.36 kW_e over the monitoring period.

393 In contrast, the DHW heater in the living wing was frequently activated throughout the day, and especially
394 in the morning during breakfast and cleaning activities. The power factor remained 1 when the heater operated
395 continuously, but dropped to a low value during the start/stop. Over the entire monitoring period, the kitchen
396 DHW heater operated for an average of 5.77 hours per day, with an average power factor of 0.95. The total
397 energy consumption for this heater was 236.88 kW_e.

398 Table 2 provides an overview of the total energy consumption in both the scientific and the principal modules
399 of GdC station during the monitoring period, spanning from February 15th to March 14th. The table highlights
400 that the total energy consumption for heating purposes is significantly higher compared to DHW purposes.
401 Specifically, the heating of the living wing emerges as the largest energy consumer, consuming a total of
402 103.5 kWh/m² over the course of 28 days. This consumption level, observed during one month of monitoring,
403 is nearly on par with the average yearly energy consumption for space heating in the European Union [48]
404 and in Canada [49].

405 **Table 2.** Total energy consumption during the four weeks monitoring period.

Module	Equipment	Time per day in use [h/d]	Mean power factor ϕ [-]	Energy consumption [kWh]	Heating consumption per square meter [kWh/m ²]
Scientific module (90 m ²)	Portable electric fan heater	12.92	1.00	1,707.90	18.98
	Electric heaters	17.85	0.55	733.62	8.15
	TOTAL HEATING			2,441.52	27.13
Living wing (120 m ²)	Furnace's fan	17.15	0.80	130.18	1.08
	Gasoil consumption	17.15	-	12,293.05	102.44
	TOTAL HEATING			12,423.22	103.53
	TOTAL DHW	5.77	0.95	236.88	-
Bedroom wing (120 m ²)	Furnace's fan	6.52	0.68	50.15	0.42
	Gasoil consumption	6.52	-	4,674.01	38.95
	TOTAL HEATING			4,724.16	39.37
	TOTAL DHW	3.77	1.00	531.36	-
TOTAL			20,357.15	170.02	

406 *3.3. CHARACTERIZATION OF THE THERMAL ENVELOPE*

407 The measurement of wall transmittance, surface temperatures, and the blower door test, in conjunction with
 408 thermography analysis, enabled the characterization of the condition of the insulation materials and the
 409 connections between the different panels. The methodology employed for this analysis is described in Section
 410 2.3. Table 3 provides the walls transmittance and air infiltration values measured at both the scientific and
 411 the principal modules. These are compared with the values specified in the Spanish Technical Building Code
 412 (CTE, for its acronym in Spanish), in which the Basic Document for Energy Saving (DB-HE) is framed [50],
 413 and with the “Passive house” and “EnerPHit” energy standards [51].

414 Based on the data presented in Table 3, it can be observed that all the measured values of wall transmittance
 415 exceed the maximum allowed limit in Spain for its most severe winter climatic zone. It's worth noting that
 416 this zone is notably milder than a polar climate, but the transmittance value in the living room are triple the
 417 permissible limit. Furthermore, when compared to the standard for passive house buildings in arctic climate
 418 zone, the living wing exceeds its maximum value by a factor of 14, the bedroom wing by a factor of 7.5, and
 419 the scientific module by a factor of 9.5.

420 Two reasons may explain why the living wing exhibits the worst result. Firstly, the living wing was
 421 repurposed after being originally used in Spain, while the scientific module and bedroom wing were purpose-
 422 built for use in Antarctica. Secondly, as depicted in the thermographic images (see Figure 15), the insulation
 423 of the living area shows significant degradation, particularly in the lower area and near the joints. This issue
 424 is particularly pronounced in the facade facing the bay, as can be observed in the thermography image in
 425 Figure 15, where a lower strip approximately 60 cm in height along the entire module appears in a much
 426 more yellow color. This can be attributed to the orientation of the bay-facing facade, which is exposed to

427 strong winds and experiences high temperature gradients between the exterior and the interior. This creates
 428 substantial pressure differences, leading to increased water infiltration, subsequent condensation in the
 429 insulators materials and, finally, their degradation with time. The continuous strip of approximately 60 cm at
 430 the bottom is mainly attributed to moisture on the lower part of the wall.

431 **Table 3.** Comparison between reference and measured values of the buildings' thermal envelope.

Ref. values / Case study	U-value opaque envelope (W/m ² K)	Air leaks at 50 Pa (h ⁻¹)	Maximum heating demand (kWh/m ²)	Thermal bridges ^a
CTE DB-HE [50]	<0.37 For climatic zone E ^b	< 6 For compactness below 2 m ³ /m ²	10 + 8 · C _{int} Non-renewable primary energy consumption	-
Passive house & EnerPHit [51]	< 0.09 For arctic climate zone	< 0.6	< 15 (for 1 year)	< 4 K
Scientific module	0.86	8.63	27.1 (for 28 days)	9 K
Living wing	1.30	6.14	103.5 (for 28 days)	10 K
Bedroom wing	0.69	4.13	39.4 (for 28 days)	8 K

^a Maximum temperature difference between the surface of the enclosure and the operating temperature.
^b For each wall in contact with exterior air.
 C_{int} = Internal heat gains [W/m²]

432

433 Through thermography analysis, we may also confirmed the presence of thermal bridges at the panel joints
 434 and at connections with the floor and ceiling (see Figure 16 and Figure 17), with the largest thermal bridge
 435 occurring at junction with the ceiling. However, the most significant issue in terms of heat loss is attributed
 436 to the windows, which have aluminum frames with high transmittance and poor airtightness. The main air
 437 infiltrations are observed at the junction between the glass and the window frames, primarily due to the
 438 degradation of the spacer sealing. As a result of this degradation, moisture enters the interior of the air gap,
 439 leading to its deterioration and adversely affecting the glass treatment.

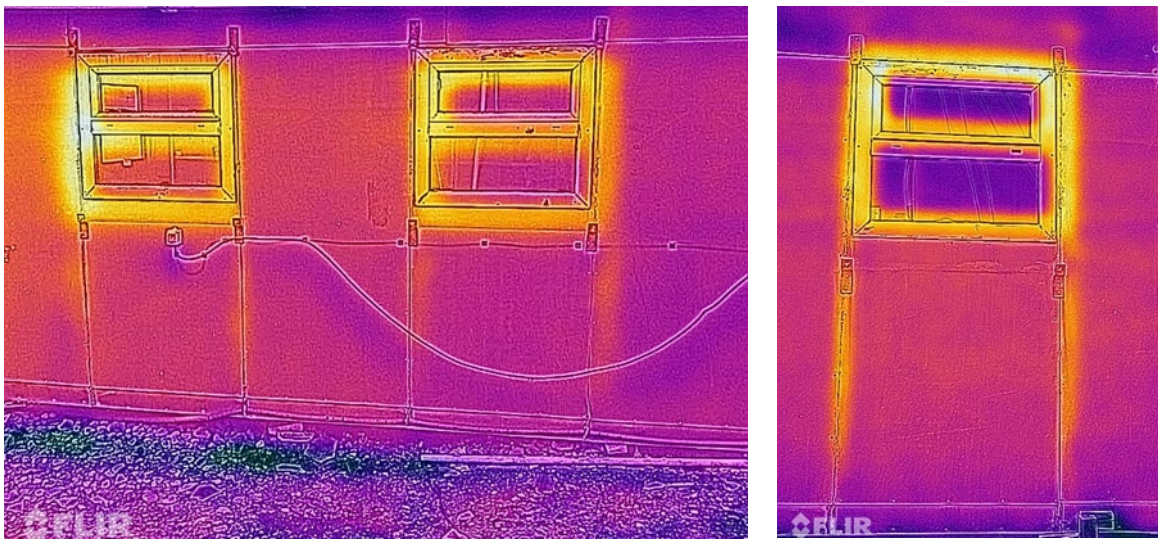
440 With a building compactness (volume/total envelope area) lower than two, Spanish regulation requires a
 441 maximum air tightness level of 3 renovations per hour and the passive house standard sets a maximum of 0.6
 442 renovation per hour, both measured at a pressure of 50 Pa. However, as indicated in Table 3, the blower door
 443 tests resulted in air renovation rates ranging from 4.1 to 8.6 air changes per hour at a pressure of 50 Pa, which
 444 are far above threshold values. In general, there were high air infiltrations in all the modules at all joints.

445 Based on these results, it is clear that the thermal envelope of the modules is in a deteriorate state, resulting
 446 in high-energy consumption for heating. The lack of thermal inertia and high permeability of the constructions
 447 necessitate continuous heater operation (especially during nights) to maintain indoor temperatures. If heating
 448 systems turned off at night, it takes several hours the following day to reach a comfortable temperature,
 449 indicating the modules' low thermal performance.



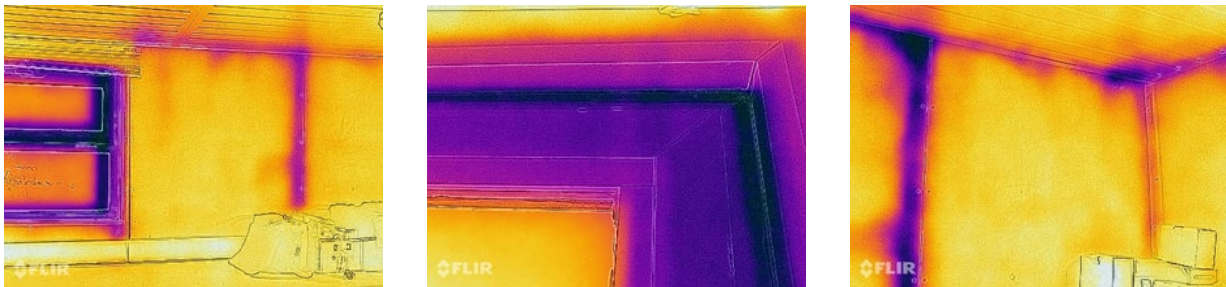
450
451

Figure 15. Exterior thermography of the living wing: deterioration of frontal wall insulation.



452

Figure 16. Exterior thermography of the scientific module.



453

Figure 17. Interior thermography of the scientific module during the blower door test.

454 4. CONCLUSIONS

455 This paper investigates the energy consumption and indoor air conditions of two buildings or modules at the
456 scientific station Gabriel de Castilla, located on Deception Island in the Antarctic continent. The data was
457 collected over a four-weeks period during the Antarctic summer and included the energy consumption for
458 heating and domestic hot water, as well as indoor air temperature, relative humidity, and CO₂ concentration.
459 Outdoor conditions were retrieved from the autonomous meteorological station operating throughout the year
460 at the station. Furthermore, by simultaneously measuring the walls' transmittance, assessing air leakages, and

461 conducting thermography analysis, it was possible to determine the actual state of conservation of the
462 buildings' enclosures without the need for any intervention or invasive techniques.

463 Overall, our findings highlight the poor condition of the thermal envelopes in both modules and the
464 inadequate performance of the heating systems. The present study not only provides insight into the starting
465 point for potential rehabilitation of these buildings but also enables proposals for improvements in future
466 constructions. Specifically, the focus should be on enhancing insulation, thermal inertia and air tightness of
467 the modules. Simultaneously, it is essential to implement an appropriate ventilation strategy to ensure
468 occupants have a healthy and controlled air supply. Considering the climatic zone (high humidity saturation
469 of the air, strong winds and high salinity), specific attention should be given to the construction materials and
470 techniques, as well as air conditioning installations. In particular, we recommend to use low-porosity
471 enclosures and high-performance windows with desiccant spacers and anti-corrosion treatments. It is also
472 considered advisable to use enthalpy heat recovery systems with preheating resistance, and aerothermal
473 systems with compact units. Finally, on-site energy production using renewable sources should be prioritized,
474 once higher energy efficiency is reached in the modules. This would have a positive impact on the carbon
475 footprint and fuel logistics, which are critical aspects for any Antarctic station.

476 It can therefore be seen that the specific climatic characteristics of Antarctica condition the buildings' design,
477 construction techniques, type of sealing and selection of materials. These cannot be extrapolated from other
478 places, since it would result in the appearance of serious buildings pathologies.

479 Antarctic research stations are a unique opportunity for investigation, and we cannot allow these studies to
480 cause irreparable damage to the continent. In this paper, we shown that energy consumption at the GdC
481 Antarctic station is much higher than the average consumption in other countries, and even twelve times
482 higher than the Passivhaus standard. Due to the serious consequences that greenhouse gas emissions have for
483 the environment, and the heat release has on the permafrost thawing, it is urgent to reach an agreement for
484 regulating the operation of bases in the Antarctic continent. Common regulations should be agreed, to set
485 high-level requirements for buildings' construction and quantifiable limits for energy consumption at bases.
486 To achieve this, it would be advisable to have guides on good construction practices for a climate as extreme
487 and complicated as Antarctica. For the creation of these guides, studies such as the one carried out in this
488 paper are necessary.

489 **CRedit authorship contribution statement**

490 **Beatriz Rodríguez Soria:** Conceptualization, Methodology, Formal analysis, Investigation, Writing –
491 review & editing, Supervision. **Miguel Ángel García García:** Conceptualization, Methodology,
492 Visualization, Writing – review & editing. **Adeline Rezeau:** Formal analysis, Data curation, Writing –
493 original draft.

494 **Declaration of Competing Interest**

495 The authors declare that they have no known competing financial interests or personal relationships that could
496 have appeared to influence the work reported in this paper.

497 **Data availability**

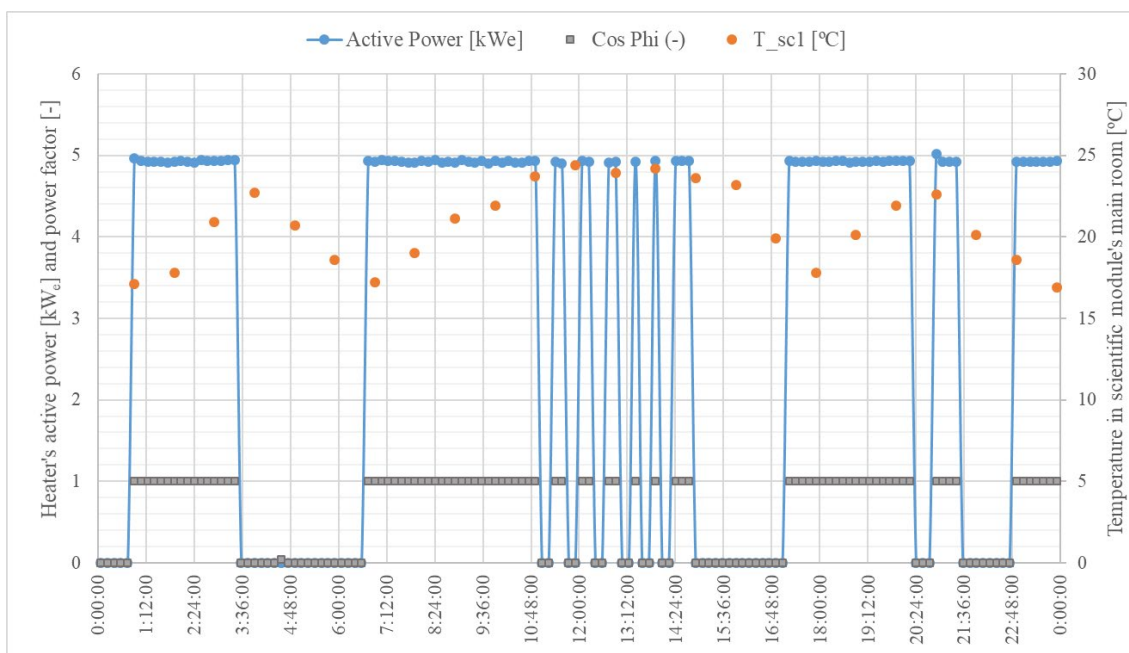
498 The authors do not have permission to share the data.

499 **Acknowledgements**

500 This project has been funded by the University Defence Center (CUD) through the Research Project CUD
501 200-15: “Energy monitoring and characterization of the Gabriel de Castilla Base” and by the European
502 Regional Development Fund “Building Europe from Aragon”, from the GITSE group of the I3A Research
503 Institute, within the line: “Modeling, simulation and design of thermal equipment and buildings”.

504 We express our gratitude to the Spanish Ministry of Defence for their support in covering travel and
505 subsistence expenses, and we extend our thanks to the staff members of the Spanish Army's XXXII Antarctic
506 Campaign for their unwavering collaboration.

507 **Appendix**



508

509 Figure A1. Operation profile of the electric fan heater and indoor temperature in the scientific module, on
510 February 24th.

511 **References**

- 512 [1] United Nations, “Kyoto Protocol to The United Nations Framework Convention on Climate Change,”
513 1998.
- 514 [2] “Council Decision of 25 April 2002 concerning the approval, on behalf of the European Community,

- 515 of the Kyoto Protocol to the United Nations Framework Convention on Climate Change and the joint
516 fulfilment of commitments thereunder (2002/658/CE).” .
- 517 [3] S. Vijayavenkataraman, S. Iniyar, and R. Goic, “A review of climate change, mitigation and
518 adaptation,” *Renew. Sustain. Energy Rev.*, vol. 16, no. 1, pp. 878–897, 2012, doi:
519 10.1016/j.rser.2011.09.009.
- 520 [4] United Nations, “Doha Amendment to the Kyoto Protocol, ref. C.N.718.2012.TREATIES-
521 XXVII.7.c,.” Doha (Qatar), 2012.
- 522 [5] United Nations Framework Convention on Climate Change, “Adoption of the Paris Agreement
523 (FCCC/CP/2015/L.9/Rev.1).” Paris (France), 2015.
- 524 [6] “Marrakech Action Proclamation for Our Climate and Sustainable Development.” Marrakech
525 (Morocco), 2016.
- 526 [7] United States Department of State, “The Long-Term Strategy of the United States: Pathways to Net-
527 Zero Greenhouse Gas Emissions by 2050.” pp. 1–63, 2021.
- 528 [8] American Planning Association (APA), “Climate Change Policy Guide,” 2020.
- 529 [9] Commission of the European Communities, “Green Paper - A European Strategy for Sustainable,
530 Competitive and Secure Energy COM(2006) 105 final,” Brussels, 2006.
- 531 [10] European Commission, “A Clean Planet for all - A European strategic long-term vision for a
532 prosperous, modern, competitive and climate neutral economy, COM(2018) 773 final,” Brussels,
533 2018.
- 534 [11] European Commission, “The European Green Deal, COM(2019) 640 final,” Brussels, 2019.
- 535 [12] United Nations, “Climate Action - All about the NDCs.” [https://www.un.org/en/climatechange/all-
536 about-ndcs](https://www.un.org/en/climatechange/all-about-ndcs) (accessed Dec. 04, 2023).
- 537 [13] G. Wendler, B. Moore, D. Dissing, and J. Kelley, “On the radiation characteristics of Antarctic sea
538 ice,” *Atmos. - Ocean*, vol. 38, no. 2, pp. 349–366, 2000, doi: 10.1080/07055900.2000.9649652.
- 539 [14] J. Turner *et al.*, “Antarctic climate change and the environment: An update,” *Polar Rec. (Gr. Brit.)*,
540 vol. 50, no. 3, pp. 237–259, 2014, doi: 10.1017/S0032247413000296.
- 541 [15] M. P. Chidichimo *et al.*, “Energetic overturning flows, dynamic interocean exchanges, and ocean
542 warming observed in the South Atlantic,” *Commun. Earth Environ.*, vol. 4, no. 1, 2023, doi:
543 10.1038/s43247-022-00644-x.
- 544 [16] F. Hrbáček *et al.*, “Active layer and permafrost thermal regimes in the ice-free areas of Antarctica,”
545 *Earth-Science Rev.*, vol. 242, no. May, 2023, doi: 10.1016/j.earscirev.2023.104458.
- 546 [17] A. Hamm, R. Magnússon, A. J. Khattak, and A. Frampton, “Continentality determines warming or
547 cooling impact of heavy rainfall events on permafrost,” *Nat. Commun.*, vol. 14, no. 1, pp. 1–13, 2023,
548 doi: 10.1038/s41467-023-39325-4.
- 549 [18] M. Mu *et al.*, “Carbon loss and emissions within a permafrost collapse chronosequence,” *Catena*, vol.
550 231, no. May, p. 107291, 2023, doi: 10.1016/j.catena.2023.107291.
- 551 [19] Secretariat of the Antarctic Treaty, “Protocol on Environmental Protection to the Antarctic Treaty (the

- 552 Madrid Protocol).” 1991.
- 553 [20] “The Antarctic Treaty,” in *Conference on Antarctica*, 1959, p. 53.
- 554 [21] CCAMLR, “Convention on the Conservation of Antarctic Marine Living Resources.” Canberra
555 (Australia), 1980.
- 556 [22] Australian Antarctic Programme, “Anstralian Antarctic Strategy and 20 year action plan.” Australian
557 Government, Canberra (Australia), 2016.
- 558 [23] “Directrices para una Estrategia Polar Española - Guidelines for a Spanish Polar Strategy,” Madrid.
- 559 [24] M. A. de Pablo, A. Molina, C. Recio, M. Ramos, G. Goyanes, and M. A. Roperro, “Análisis del estado
560 de la capa activa en el emplazamiento de la base antártica española Gabriel de Castilla, Isla Decepción,
561 Antártida,” *Boletín Geológico y Min.*, vol. 128, no. 1, pp. 69–92, Mar. 2017, doi:
562 10.21701/bolgeomin.128.1.004.
- 563 [25] Antarctic Treaty Nations, “Deception Island Management Package,” Stockholm, Sweden, 2005.
- 564 [26] T. Tin *et al.*, “Energy efficiency and renewable energy under extreme conditions: Case studies from
565 Antarctica,” *Renew. Energy*, vol. 35, no. 8, pp. 1715–1723, 2010, doi: 10.1016/j.renene.2009.10.020.
- 566 [27] S. T. Brooks, “Developing a standardised approach to measuring the environmental footprint of
567 antarctic research stations,” *J. Environ. Assess. Policy Manag.*, vol. 16, no. 4, 2014, doi:
568 10.1142/S1464333214500379.
- 569 [28] E. Crossin, K. Verghese, S. Lockrey, H. Ha, and G. Young, “The environmental impacts of operating
570 an Antarctic research station,” *J. Ind. Ecol.*, vol. 24, no. 4, pp. 791–803, 2020, doi: 10.1111/jiec.12972.
- 571 [29] H. Yoshino, T. Hong, and N. Nord, “IEA EBC annex 53: Total energy use in buildings—Analysis
572 and evaluation methods,” *Energy Build.*, vol. 152, pp. 124–136, Oct. 2017, doi:
573 10.1016/j.enbuild.2017.07.038.
- 574 [30] M. Aksoezen, M. Daniel, U. Hassler, and N. Kohler, “Building age as an indicator for energy
575 consumption,” *Energy Build.*, vol. 87, pp. 74–86, Jan. 2015, doi: 10.1016/j.enbuild.2014.10.074.
- 576 [31] Creative Commons, “Deception Island Map,” 2018. .
- 577 [32] “Directive Plan of ‘Gabriel de Castilla’ station.” Infrastructure Direction, Spanish Ministry of
578 Defense, 2012.
- 579 [33] Spanish State Meteorological Agency (AEMET), “Informe climatológico de las Bases Antárticas
580 Españolas 2020.”
- 581 [34] K. L. Smith, R. J. Baldwin, R. C. Glatts, T. K. Chereskin, H. Ruhl, and V. Lagun, “Weather, ice, and
582 snow conditions at Deception Island, Antarctica: long time-series photographic monitoring,” *Deep
583 Sea Res. Part II Top. Stud. Oceanogr.*, vol. 50, no. 10–11, pp. 1649–1664, Jun. 2003, doi:
584 10.1016/S0967-0645(03)00084-5.
- 585 [35] “ISO 9972:2015 Thermal performance of buildings - Determination of air permeability of buildings -
586 Fan pressurization method.”
- 587 [36] Gobierno de España, “Royal Decree 1027/2007 that adopts the Regulations for Thermal Installations
588 in Buildings,” *Boletín Of. del Estado*, p. 54, 2007.

- 589 [37] Gobierno de España, “Royal Decree 178/2021, of March 23, which modifies Royal Decree 1027/2007,
590 of July 20, approving the Regulation of Thermal Installations in Buildings.,” *Boletín Of. del Estado*,
591 pp. 61561–61567, 2021.
- 592 [38] European Norm, “EN 16798 -1 Energy performance of buildings. Ventilation for buildings. Part 1:
593 Indoor environmental input parameteres for design and assessment of energy performance of
594 buildings addressing indoor air quality, thermal environment, lighting and acoustics.,” 2019.
- 595 [39] P. Wolkoff, “Indoor air humidity, air quality, and health – An overview,” *Int. J. Hyg. Environ. Health*,
596 vol. 221, no. 3, pp. 376–390, 2018, doi: 10.1016/j.ijheh.2018.01.015.
- 597 [40] S. Urlaub and G. Grün, “Fraunhofer-Institut für Bauphysik IBP report. Mould and dampness in
598 European homes and their impact on health,” 2016.
- 599 [41] World Health Organization, *WHO guidelines for indoor air quality: dampness and mould*. 2009.
- 600 [42] M. J. Mendell, J. M. Macher, and K. Kumagai, “Measured moisture in buildings and adverse health
601 effects: A review,” *Indoor Air*, vol. 28, no. 4, pp. 488–499, 2018, doi: 10.1111/ina.12464.
- 602 [43] Y. Xue, Y. Fan, Z. Wang, W. Gao, Z. Sun, and J. Ge, “Facilitator of moisture accumulation in building
603 envelopes and its influences on condensation and mould growth,” *Energy Build.*, vol. 277, p. 112528,
604 2022, doi: 10.1016/j.enbuild.2022.112528.
- 605 [44] X. Zhang, P. Wargocki, and Z. Lian, “Physiological responses during exposure to carbon dioxide and
606 bioeffluents at levels typically occurring indoors,” *Indoor Air*, vol. 27, no. 1, pp. 65–77, Jan. 2017,
607 doi: 10.1111/INA.12286.
- 608 [45] S. Shriram, K. Ramamurthy, and S. Ramakrishnan, “Effect of occupant-induced indoor CO2
609 concentration and bioeffluents on human physiology using a spirometric test,” *Build. Environ.*, vol.
610 149, pp. 58–67, Feb. 2019, doi: 10.1016/J.BUILDENV.2018.12.015.
- 611 [46] D. P. Wyon, “The effects of indoor air quality on performance and productivity,” *Indoor Air, Suppl.*,
612 vol. 14, no. SUPPL. 7, pp. 92–101, 2004, doi: 10.1111/J.1600-0668.2004.00278.X.
- 613 [47] ASHRAE Board of Directors, “ASHRAE Position Document on Indoor Carbon Dioxide,” p. 17, 2022.
- 614 [48] ODYSSEE-MURE, “European Union - Energy efficiency trends and policies.” p. 10, 2021.
- 615 [49] International Energy Agency (IEA), “Heating and Cooling Strategies in the Clean Energy Transition,”
616 *Outlooks and lessons from Canada’s provinces and territories*. 2019.
- 617 [50] Gobierno de España, “Royal Decree 450/2022, of June 14, amending the Technical Building Code,
618 approved by Royal Decree 314/2006, of March 17,” *Boletín Of. del Estado*, pp. 61561–61567, 2022.
- 619 [51] Passive House Institute, “Criteria for Buildings. Passive House - EnerPHit - PHI Low Energy
620 Building. Versión 10c,” no. January, p. 131, 2023.
- 621